

Synthesis and Molecular Structures of Mononitrosyl (N₂S₂)M(NO) Complexes (M = Fe, Co)

Chao-Yi Chiang, Jonghyuk Lee, Christopher Dalrymple, Michael C. Sarahan, Joseph H. Reibenspies, and Marcetta Y. Darensbourg*

Department of Chemistry, Texas A&M University, College Station, Texas 77843

Received June 22, 2005

A series of tetragonally distorted square pyramids of formula N₂S₂M(NO) (M = Fe, Co) is prepared and characterized by $\nu(\text{NO})$ IR and EPR spectroscopies, magnetism and electrochemical properties, as well as solid-state crystal structure determinations. While the $\nu(\text{NO})$ IR frequencies and the $\angle\text{M}-\text{N}-\text{O}$ angles indicate differences in the electronic environment of NO consistent with the Enemark–Feltham notation of {Fe(NO)}⁷ and {Co(NO)}⁸, the reduction potentials, assigned to {Fe(NO)}⁷ + e⁻ ⇌ {Fe(NO)}⁸ and {Co(NO)}⁸ + e⁻ ⇌ {Co(NO)}⁹ respectively, are very similar, and in cases identical, for most members of the series. Coupled with the potential for the M(NO) units to breathe out of and into the N₂S₂ core plane are unique S–M–N–O torsional arrangements and concomitant π -bonding interactions which may account for the unusual coherence of reduction potentials within the series.

Introduction

The chemical properties and reactivity of transition metal–N₂S₂ complexes have been well studied, utilizing a variety of metal ions such as Fe^{II}, Ni^{II}, Pd^{II}, Co^{II}, Cu^{II}, and Zn^{II} with a host of N₂S₂ ligands.^{1–5} Open-chain tetradentate N₂S₂ ligands, as well as those based on diazacycles and other restricted donor atom connectors, typically adopt a square planar configuration when coordinated to d⁸ metals such as

Ni²⁺ and Pd²⁺.² Examples of planar N₂S₂Cu(II) complexes are also known.⁶ With Fe²⁺ and Co²⁺, penta-coordination results from dimerization of N₂S₂M units or from addition of another ligand, as in N₂S₂Fe(NO).⁴ In addition, an alternate conformation permits such N₂S₂ ligands to serve as bidentate ligands, binding only through thiolate sulfurs to form tetrahedral complexes such as in (RS)₂Fe(NO)₂⁻, the dinitrosyl iron complexes, or DNIC⁺s.^{7,8}

The reaction chemistry of N₂S₂Ni derivatives have received attention particularly since the nucleophilicity of the cis-dithiolates toward a great variety of electrophiles has produced stable complexes which maintain the Ni–S connections. Reactions of electrophiles with [N₂S₂Fe]₂ complexes are not as accommodating as with the nickel derivatives, and where reactions are readily interpreted, the sites are different. For example, dioxygen reacts with N₂S₂–

* To whom correspondence should be addressed. E-mail: marcetta@mail.chem.tamu.edu. Fax: (979) 845-0158.

- (1) (a) Kovacs, J. A. *Chem. Rev.* **2004**, *104*, 825–848 and references therein. (b) Harrop, T. C.; Mascharak, P. K. *Acc. Chem. Res.* **2004**, *37*, 253–260 and references therein. (c) Artaud, I.; Chatel, S.; Chauvin, A. S.; Bonnet, D.; Kopf, M. A.; Leduc, P. *Coord. Chem. Rev.* **1999**, *190–192*, 577–586 and references therein. (d) Heinrich, L.; Li, Y.; Vaissermann, J.; Chottard, J.-C. *Eur. J. Inorg. Chem.* **2001**, 1407–1409.
- (2) (a) Taylor, M. K.; Reglinski, J.; Wallace, D. *Polyhedron* **2004**, *23*, 3201–3209. (b) Jicha, D. C.; Busch, D. H. *Inorg. Chem.* **1962**, *1*, 872–877. (c) Thompson, M. C.; Busch, D. H. *J. Am. Chem. Soc.* **1964**, *86*, 3651–3656.
- (3) (a) Golden, M. L.; Reibenspies, J. H.; Darensbourg, M. Y. *Inorg. Chem.* **2004**, *43*, 5798–5800. (b) Golden, M. L.; Jeffery, S. P.; Miller, M. L.; Reibenspies, J. H.; Darensbourg, M. Y. *Eur. J. Inorg. Chem.* **2004**, 231–236. (c) Golden, M. L.; Rampersad, M. V.; Reibenspies, J. H.; Darensbourg, M. Y. *Chem. Commun.* **2003**, 1824–1825. (d) Bellefeuille, J. A.; Grapperhaus, C. A.; Buonomo, R. M.; Reibenspies, J. H.; Darensbourg, M. Y. *Organometallics* **1998**, *17*, 4813–4821. (e) Musie, G.; Lai, C.-H.; Reibenspies, J. H.; Sumner, L. W.; Darensbourg, M. Y. *Inorg. Chem.* **1998**, *37*, 4086–4093. (f) Grapperhaus, C. A.; Darensbourg, M. Y. *Acc. Chem. Res.* **1998**, *31*, 451–459 and references therein. (g) Mills, D. K.; Hsiao, Y. M.; Farmer, P. J.; Atnip, E. V.; Reibenspies, J. H.; Darensbourg, Y. D. *J. Am. Chem. Soc.* **1991**, *113*, 1421–1423.

- (4) (a) Krüger, H.-J.; Holm, R. H. *Inorg. Chem.* **1987**, *26*, 3645–3647. (b) Krüger, H.-J.; Peng, G.; Holm, R. H. *Inorg. Chem.* **1991**, *30*, 734–742. (c) Rao, P. V.; Bhaduri, S.; Jiang, J.; Hong, D.; Holm, R. H. *J. Am. Chem. Soc.* **2005**, *127*, 1933–1945 and references therein. (d) Rao, P. V.; Bhaduri, S.; Jiang, J.; Holm, R. H. *Inorg. Chem.* **2004**, *43*, 5833–5849 and references therein. (e) Patterson, G. S.; Holm, R. H. *Bioinorg. Chem.* **1975**, *4*, 257–275.
- (5) (a) Rabinowitz, H. N.; Karlin, K. D.; Lippard, S. J. *J. Am. Chem. Soc.* **1977**, *99*, 1420–1426. (b) Karlin, K. D.; Lippard, S. J. *J. Am. Chem. Soc.* **1976**, *98*, 6951–6957.
- (6) Hanss, J.; Krüger, H.-J. *Angew. Chem., Int. Ed. Engl.* **1996**, *35*, 2827–2830.
- (7) Baltusis, L. M.; Karlin, K. D.; Rabinowitz, H. N.; Dewan, J. C.; Lippard, S. J. *Inorg. Chem.* **1980**, *19*, 2627–2632.
- (8) Chiang, C.-Y.; Miller, M. L.; Reibenspies, J. H.; Darensbourg, M. Y. *J. Am. Chem. Soc.* **2004**, *126*, 10867–10874.

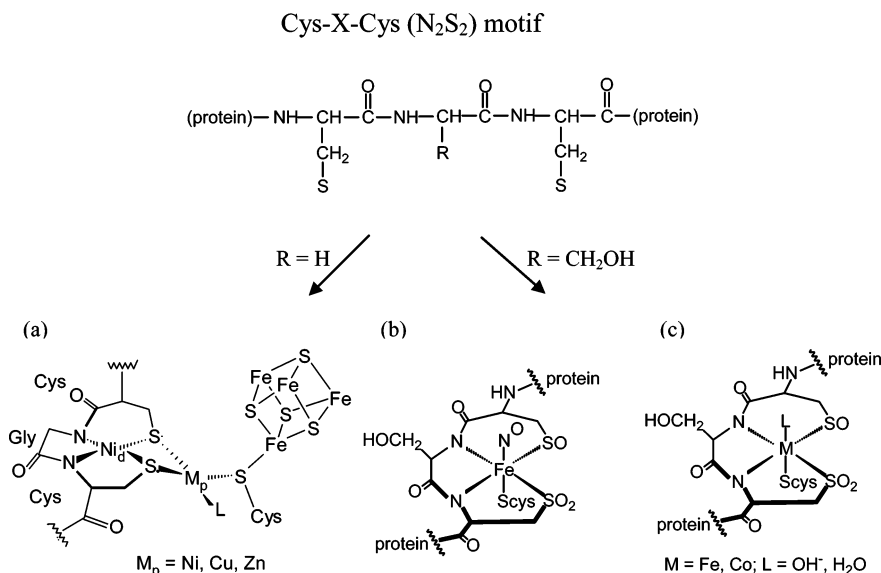


Figure 1. Cys–X–Cys (N_2S_2) motif and its metal complexes in biological systems. Active site of (a) ACS in *Moorella thermoacetica*;⁹ (b) NO-inactive form of Fe–NHase in *Rhodococcus* sp. N-771;^{10c} (c) Fe–NHase in *Rhodococcus* R312 and Co–NHase in *Pseudonocardia thermophila* JCM 3095.^{10a,10b}

Ni to produce nickel-bound S-oxygenates;^{3(f)} with $[N_2S_2Fe]_2$ complexes, the μ -oxo-diiron(III) derivatives are obtained.^{3(e)}

With such an extensive display of N_2S_2M examples (up to 300 square planar N_2S_2M “hits” may be found in the Cambridge Data Base of Crystallographic Structures), the revelation that such a binding motif exists in metalloproteins such as the active sites of acetyl-coA synthase (ACS) and nitrile hydratase (NHase) came with a considerable chemical history. These active sites demonstrate that a Cys–X–Cys protein backbone motif can be used to provide two nitrogens and two cysteinyl sulfurs of the tetraanionic N_2S_2 binding site, Figure 1.^{9,10} Appropriate to this report is nitrile hydratase which finds that iron or cobalt resides in a Cys–Ser–Cys (S–N–N–S) tripeptide motif. Another proteinyl cysteine coordinates to a fifth position of the octahedral metal center, and in the as-isolated, deactivated form, an NO binds trans to that cysteinyl sulfur.¹⁰ The two cysteinyl sulfurs in the N_2S_2 tripeptide are found as S-oxygenates, generated in a post-translational modification into sulfinate (RSO_2^-) and sulfenate (RSO^-) moieties.¹⁰ Photochemical activation removes the NO and produces the active form which has a hydroxide or water ligand in the sixth site (Figure 1). The Co structure is reported to be analogous to the iron structure in the activated NHase;^{1a,1b,10a} the NO-deactivated form is unknown for cobalt.

Several model complexes have produced aspects of the first coordination sphere donor environment about iron and cobalt in nitrile hydratase.¹ Our experience with specific dianionic N_2S_2 ligands based on mesocyclic diazacycloalkane

moieties as N-to-N connectors, bismercaptoethanediazacyclohexane and bismercaptoethanediazacycloheptane, bme-daco, and bme-dach, respectively, led us to examine nickel derivatives as small molecule models of the distal nickel of the ACS active sites.³ As analogues to the nickel complexes and as reaction products in the transfer of NO from the DNIC complex⁸ described above, $(N_2S_2)Fe(NO)$ and $(N_2S_2)Co(NO)$ derivatives have been prepared. Their characterization by X-ray crystallography, $\nu(NO)$ stretching frequencies, EPR, and cyclic voltammetry have revealed interesting properties, particularly as this set of donor atoms might compare to the N_4 donor set of porphyrinic ligands. While never as ubiquitous as the porphyrin ligand, the N_2S_2 donor set from Cys–X–Cys could be a pervasive metal-binding motif in nature. With this in mind, we present our studies below.

Experimental Section

Materials and Techniques. Syntheses and manipulations were performed using standard Schlenk-line and syringe/rubber septa techniques under N_2 or in an argon atmosphere glovebox. Filtrations of solutions used airless-ware glass frits, typically with 1–2 cm pads of Celite. Solvents were of reagent grade and purified as follows. Dichloromethane was distilled over P_4O_{10} under N_2 . Acetonitrile was distilled once from CaH_2 , once from P_4O_{10} , and freshly distilled from CaH_2 immediately before use. Diethyl ether, toluene, THF, and hexane were distilled from sodium/benzophenone under N_2 . Syntheses of N,N' -bis(2-mercaptoethyl)-1,5-diazacyclooctane ($H_2bme-daco$),¹¹ N,N' -bis(2-methyl-2-mercaptoethyl)-1,5-diazacyclooctane (H_2bme^*-daco),¹¹ N,N' -bis(2-mercaptoethyl)-1,5-diazacycloheptane ($H_2bme-dach$),¹² N,N' -dimethyl- N,N' -bis(2-mercaptoethyl)-1,3-propanediamine ($H_2bme-pda$),^{5b} and their iron or cobalt complexes, $[(bme-daco)Fe]_2^{3+}$ and its NO derivative, (bme-

(9) (a) Doukov, T. I.; Iverson, T. M.; Seravalli, J.; Ragsdale, S. W.; Drennan, C. L. *Science* **2002**, *298*, 567–572. (b) Darnault, C.; Vollbeda, A.; Kim, E. J.; Legrand, P.; Vernède, X.; Lindahl, P. A.; Fontecilla-Camps, J. C. *Nat. Struct. Biol.* **2003**, *10*, 271–279.

(10) (a) Miyanaga, A.; Fushinobu, S.; Ito, K.; Wakagi, T. *Biochim. Biophys. Res. Commun.* **2001**, *288*, 1169–1174. (b) Huang, W.; Jia, J.; Cummings, J.; Nelson, M.; Schneider, G.; Lindqvist, Y. *Structure* **1997**, *5*(5), 691–699. (c) Nagashima, S.; Nakasako, M.; Dohmae, N.; Tsujimura, M.; Takio, K.; Odaka, M.; Yohda, M.; Kamiya, N.; Endo, I. *Nat. Struct. Biol.* **1998**, *5*, 347–351.

(11) Mills, D. K.; Font, I.; Farmer, P. J.; Tuntulani, T.; Buonomo, R. M.; Goodman, D. C.; Musie, G.; Grapperhaus, C. A.; Maguire, M. J.; Lai, C.-H.; Hatley, M. L.; Smees, J. J.; Bellefeuille, J. A.; Darenbourg, M. Y. *Inorg. Synth.* **1998**, *32*, 89–98.

(12) Smees, J. J.; Miller, M. L.; Grapperhaus, C. A.; Reibenspies, J. H.; Darenbourg, M. Y. *Inorg. Chem.* **2001**, *40*, 3601–3605.

daco)Fe(NO) (complex **1**),⁸ [(bme*-daco)Fe]₂,^{3c} [(bme-dach)Fe]₂,¹³ and [(bme-pda)Co]₂^{5a} were according to published procedures. S-Nitroso-triphenylmethanethiol (Ph₃CSNO),¹⁴ and tetrakis(acetonitrile)copper(I) tetrafluoroborate ([Cu(CH₃CN)₄]BF₄)¹⁵ were synthesized according to published procedures. NO gas (98.5%) was purchased from Aldrich Chemical Co. and used as received.

Infrared spectra were recorded on a Mattson 6022 spectrometer in a CaF₂ cell of 0.1 mm path length. Vis/UV spectra were recorded on a Hewlett-Packard HP8452A diode array spectrophotometer. Elemental analyses were performed by Canadian Microanalytical Systems in Delta, British Columbia, Canada. Electrospray ionization mass spectrometry data were obtained at the Laboratory for Biological Mass Spectrometry, Texas A&M University, College Station, Texas using a MDS Series Qstar Pulsar with a spray voltage of 5 keV. The EPR spectrum was recorded on a Bruker X-band EPR spectrometer (model ESP 300E) with Oxford Liquid Helium/Nitrogen cryostat at 77 K in CH₂Cl₂, 1 mW power and 0.1 mT modulated amplitude.

X-Ray Structure Determinations. X-ray data were obtained on a Bruker Apex CCD diffractometer and covered a hemisphere of space by combining three frame sets of exposures. The space groups were determined on the basis of systematic absences and intensity statistics. The structures were solved by direct methods. Anisotropic displacement parameters were determined for all non-hydrogen atoms. Hydrogen atoms were added at idealized positions and refined with fixed isotropic displacement parameters equal to 1.2 (1.5 for methyl protons) times the isotropic displacement parameters of the atoms to which they were attached. Atoms which proved to be definitely nonpositive were corrected by including the command Simu with the "s" parameter set at 0.05 in the instruction file. Programs used for data collection and cell refinement, SMART;¹⁶ data reduction, SAINT-Plus;¹⁷ structure solution, SHELXS-86 (Sheldrick);¹⁸ structure refinement, SHELXL-97 (Sheldrick);¹⁹ and molecular graphics and preparation of material for publication, SHELXTL-Plus, version 5.1 or later (Bruker).²⁰

Electrochemistry. Cyclic voltammograms were recorded on a BAS-100A electrochemical analyzer using a glassy carbon disk (0.071 cm²) as the working electrode, the reference electrode was Ag/AgCl prepared by the electroplating method, and the counter electrode was a coiled platinum wire. The glassy carbon working electrode was polished with 15, 3, and 1 μm diamond pastes, successively, and then sonicated in ultrapure (Millipore) water for 10 min. Solutions were deaerated by an argon purge for 5–10 min, and a blanket of argon was maintained over the solution while performing the measurements. All experiments were performed on CH₂Cl₂ solutions containing 0.1 M *n*-Bu₄NPF₆ at room temperature. Cp*₂Fe served as internal reference since the oxidation peaks for samples were overlapped with the Cp₂Fe/Cp₂Fe⁺ redox wave. All potentials are reported relative to the Ag/AgCl electrode using Cp*₂Fe/Cp*₂Fe⁺ as a reference (*E*_{1/2} = 0.00 V vs Ag/AgCl in CH₂Cl₂). Under identical conditions, the measured potential difference

between Cp₂Fe/Cp₂Fe⁺ and Cp*₂Fe/Cp*₂Fe⁺ was 556 mV (i.e., *E*_{1/2} for Cp₂Fe/Cp₂Fe⁺ = +556 mV).

Instrumental *iR* compensation was not used to minimize uncompensated *iR* drops in the solution, and Δ*E* for redox couples were directly compared with that of the internal reference Cp*₂Fe/Cp*₂Fe⁺.²¹

Preparation of (bme*-daco)Fe(NO), Complex 2. A 0.048 g (0.70 mmol) portion of [(bme*-daco)Fe]₂ was dissolved in 30 mL of MeOH in a 100 mL Schlenk flask at 60 °C under argon. Following replacement of Ar with NO gas (1 atm), the solution color changed from purple-brown to green within 30 min. The solvent was removed under vacuum. The residue was redissolved in 50 mL of CH₂Cl₂ and filtered through Celite. The green filtrate was concentrated to 5 mL under vacuum and the addition of 30 mL of pentane resulted in precipitation of a green solid; yield 0.012 g, 23%. Green crystals of X-ray diffraction quality were obtained by diffusion of pentane vapor into a CH₂Cl₂ solution of complex **2** maintained at 5 °C. IR(ν_{NO}): 1643(s) cm⁻¹ (CH₂Cl₂). Anal. Calcd for C₁₄H₂₈ON₃FeS₂: C, 44.44; H, 8.52; N, 11.10. Found: C, 44.51; H, 7.59; N, 10.77.

Preparation of (bme-dach)Fe(NO), Complex 3. In the same manner as described above, complex **3** was prepared and isolated, however in a much better yield of 95% (1.15 g). IR(ν_{NO}): 1647(s) cm⁻¹ (CH₂Cl₂). Anal. Calcd for C₉H₁₈ON₃FeS₂: C, 35.53; H, 5.96; N, 13.81. Found: C, 34.92; H, 5.96; N, 13.26.

Preparation of [(N₂S₂)Co]₂ (N₂S₂ = bme-daco, bme*-daco, bme-dach). The diazacycle derivatives of [(N₂S₂)Co]₂ were prepared following the procedures for [(bme-pda)Co]₂.^{5a} The particular H₂N₂S₂ ligand (~3.3 g, 15 mmol) was dissolved in 50 mL of toluene followed by dropwise addition of 50 mL of a brown toluene solution of Co(acac)₂ (1.29 g, 5 mmol) at 22 °C. After being stirred for 24 h, the solution color changed to green with formation of a precipitate. The green solid was collected and washed with toluene and ether; yield, 73–86%.

Preparation of (bme-daco)Co(NO), Complex 4. (bme-daco)-Co(NO) was synthesized in a manner similar to that of (bme-daco)-Fe(NO). A 1.5 g (2.58 mmol) portion of [(bme-daco)Co]₂ was dissolved in 50 mL of MeOH under argon. Upon replacing the argon atmosphere with NO gas (1 atm), the solution color changed from black-green to purple-brown within 30 min. The solvent was removed under vacuum. The soluble portion of the residue was taken up in 50 mL of CH₂Cl₂ and filtered through Celite. The purplish-brown filtrate was concentrated to 5 mL under vacuum; addition of 30 mL of pentane resulted in precipitation of a dark brown solid, yield 1.51 g, 91.2%. IR(ν_{NO}): 1600(s) cm⁻¹ (CH₂Cl₂). Anal. Calcd for C₁₉H₁₈ON₃CoS₂: C, 37.34; H, 5.96; N, 12.43. Found: C, 37.38; H, 6.27; N, 13.08.

Preparation of (bme-pda)Co(NO), Complex 5. In same manner as described above, complex **5** was prepared and isolated; yield 1.74 g, 44.9%. IR(ν_{NO}): 1596(s) cm⁻¹ (CH₂Cl₂). Anal. Calcd for C₁₉H₁₈ON₃CoS₂: C, 34.94; H, 6.52; N, 13.58. Found: C, 33.35; H, 5.62; N, 12.85.

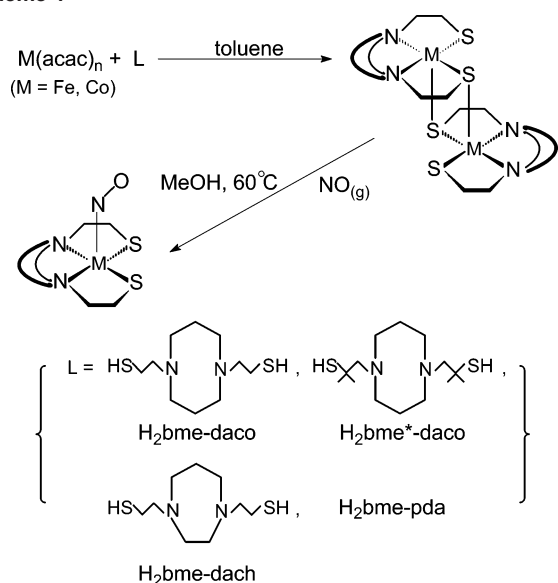
Results and Discussion

Syntheses. The direct route to (N₂S₂)M(NO) complexes is described in Scheme 1. The iron(III) acetylacetonate salt is equally efficient to Fe(II)(acac)₂ in the synthesis of the [(N₂S₂)Fe]₂ precursor since excess thiol ligand serves as sacrificial reductant. Cobalt(II) acetylacetonate is the preferred starting material for the cobalt derivatives.^{5a}

- (13) Musie, G. Ph.D. Dissertation, Texas A&M University, 1997.
 (14) Arulsamy, N.; Bohle, D. S.; Butt, J. A.; Irvine, G. J.; Jordan, P. A.; Sagan, E. *J. Am. Chem. Soc.* **1999**, *121*, 7115–7123.
 (15) Kubas, G. *J. Inorg. Synth.* **1979**, *19*, 90–92.
 (16) *Smart 1000 CCD*; Bruker Analytical X-ray Systems: Madison, WI, 1999.
 (17) *SAINT-Plus*, version 6.02; Bruker: Madison WI, 1999.
 (18) Sheldrick, G. *SHELXS-86: Program for Crystal Structure Solution*; Institut für Anorganische Chemie, Universität Göttingen: Göttingen, Germany, 1986.
 (19) Sheldrick, G. *SHELXL-97: Program for Crystal Structure Solution*; Institut für Anorganische Chemie, Universität Göttingen: Göttingen, Germany, 1997.
 (20) *SHELXTL*, version 5.1 or later; Bruker: Madison, WI, 1998.

- (21) Gagne, R. R.; Koval, C. A.; Lisensky, G. C. *Inorg. Chem.* **1980**, *19*, 2855–2857.

Scheme 1



Reddish-brown methanol solutions of dimeric $[(\text{N}_2\text{S}_2)\text{Fe}]_2$ complexes ($\text{N}_2\text{S}_2 = \text{bme-daco, bme}^*\text{-daco, bme-dach}$) were exposed to 1 atm of $\text{NO}(\text{g})$, whereupon an immediate green color developed along with a green precipitate. The green product was isolated within 30 min, otherwise extended periods led to the formation of Roussin's red ester-type products.⁸ Yields of 85–95% of the $(\text{N}_2\text{S}_2)\text{Fe}(\text{NO})$ complexes were obtained for the bme-daco and bme-dach ligands; the sterically hindered ($\text{bme}^*\text{-daco}$) $\text{Fe}(\text{NO})$ derivative led to unstable products and poorer isolated yields (20–25%).

As solids the purified $(\text{N}_2\text{S}_2)\text{Fe}(\text{NO})$ complexes are thermally and, for short periods of time, air stable. As a precaution, all solutions of metal nitrosyl complexes were maintained under N_2 or Ar. In a similar manner, complexes $(\text{N}_2\text{S}_2)\text{Co}(\text{NO})$ were gained from the highly air-sensitive, green $[(\text{N}_2\text{S}_2)\text{Co}]_2$ precursors as dark brown solids. The cobalt nitrosyl derivatives are thermally and air stable.

Spectral Characterization. $\nu(\text{NO})$ Infrared Data. Complexes **1**, (bme-daco) $\text{Fe}(\text{NO})$,⁸ **2**, ($\text{bme}^*\text{-daco}$) $\text{Fe}(\text{NO})$, and **3**, (bme-dach) $\text{Fe}(\text{NO})$, have a single $\nu(\text{NO})$ IR band at 1649, 1643, and 1647 cm^{-1} , respectively. That the gem dimethyl groups on the carbon α to the thiolate slightly increase electron density at iron, with delocalization onto the NO in complex **2** as compared to **1**, is suggested by the 6 cm^{-1} red shift in the $\nu(\text{NO})$ position. Table 1 contrasts these values to several analogous compounds. The bme-pda and bme-eda ligands, structures A and B,^{5,7,25} are open-chain analogues of the diazacycle ligands of our studies, and Lippard and co-workers have synthesized $\text{N}_2\text{S}_2\text{Fe}(\text{NO})$ derivatives of these. Artaud et al. have prepared the $[(\text{N}_2\text{S}_2)\text{Fe}(\text{NO})]^-$

Table 1. $\nu(\text{NO})$ Infrared Data (in CH_2Cl_2 Except Where Noted) and $\angle\text{M-N-O}$ of $\text{LM}(\text{NO})$ Complexes ($M = \text{Fe}$ and Co)

compound	E–F notation ²³	$\nu(\text{NO})$ cm^{-1}	$\angle\text{LM}(\text{NO})$
NHase ^a	{Fe(NO)} ⁶	1853 ²³	158.6 ^{10(c)}
[(bmb-pda)Fe(NO)] ^{-b}	{Fe(NO)} ⁶	1780 ²⁴	177.5 ²⁴
(bme-pda)Fe(NO)	{Fe(NO)} ⁷	1638 ⁷	155.2 ⁷
(bme-eda)Fe(NO)	{Fe(NO)} ⁷	1665 ²⁵	155.2 ²⁵
(bme-daco)Fe(NO), 1	{Fe(NO)} ⁷	1649 ⁸	151.7 ⁸
(bme*-daco)Fe(NO), 2 ^c	{Fe(NO)} ⁷	1643	148.7
(bme-dach)Fe(NO), 3 ^c	{Fe(NO)} ⁷	1647	152.4
(TPP)Fe(NO)	{Fe(NO)} ⁷	1675 ²⁶	144
(OEP)FeNO	{Fe(NO)} ⁷	1665 ²⁷	149.2 ³⁰
			144.4 ³¹
			142.7
(bme-daco)Co(NO), 4 ^c	{Co(NO)} ⁸	1600	129.6
			128.7
(bme*-daco)Co(NO) ^c	{Co(NO)} ⁸	1598	—
(bme-dach)Co(NO) ^c	{Co(NO)} ⁸	1600	—
(bme-pda)Co(NO), 5 ^c	{Co(NO)} ⁸	1596	130.1
			126.7
(TPP)Co(NO)	{Co(NO)} ⁸	1682 ²⁸	135.2 ³²
(OEP)Co(NO)	{Co(NO)} ⁸	1670 ²⁹	122.7 ²⁹

^a Buffer containing 50 mM HEPES–KOH (pH 7.5) and 20 mM *n*-butyric acid. ^b KBr. ^c This work.

complex of the tetraanionic bmb-pda ligand (C).²⁴ As given in Table 1, the $\nu(\text{NO})$ values of the (bme-pda) $\text{Fe}(\text{NO})$ and (bme-eda) $\text{Fe}(\text{NO})$ compounds are comparable to those of the neutral complexes **1**, **2**, and **3**, while that of the monoanionic bmb-pda complex is ca. 130 cm^{-1} higher. This high $\nu(\text{NO})$ value is consistent with the switch of the $\text{Fe}(\text{NO})$ unit into its oxidized redox level. That is, the {Fe(NO)}⁶ Enemark–Feltham (E–F) notation²³ is appropriate for the [(bmb-pda)Fe(NO)]⁻ complex and {Fe(NO)}⁷ is the assignment for the neutral complexes. The stabilization of the oxidized {Fe(NO)}⁶ by tetraanionic N_2S_2 is also seen in nitrile hydratase where the $\nu(\text{NO})$ is 1853 cm^{-1} in the Cys–Ser–Cys tripeptide motif.²³

Lower NO stretching frequencies of ca. 50 cm^{-1} for the $(\text{N}_2\text{S}_2)\text{Co}(\text{NO})$ complexes as compared to $(\text{N}_2\text{S}_2)\text{Fe}(\text{NO})$ are attributed to the greater electron-rich character of the cobalt derivatives; this is consistent with the E–F redox level notation of {Co(NO)}⁸ and {Fe(NO)}⁷, respectively. Noted for comparison in Table 1 are the $\nu(\text{NO})$ values for PM(NO) (P = TPP, OEP; M = Fe, Co) which have been assigned to the same E–F redox levels as in the N_2S_2 derivatives.^{26,27} The data show lower values for the $(\text{N}_2\text{S}_2)\text{M}(\text{NO})$ complexes as compared to PM(NO) analogues with greater discrepancies (ca. 70–80 cm^{-1}) for the cobalt complexes.^{28,29} This suggests that the dithiolate ligands of $\text{N}_2\text{S}_2^{2-}$ ligands are better electron donors than the amide (N^-) donors of the N_4^{2-} porphyrin ligands.

The (bme-daco) $\text{Fe}(\text{NO})$ compound is stable in the presence of 1 atm of NO in MeOH for about 4 h, while the ($\text{bme}^*\text{-daco}$) $\text{Fe}(\text{NO})$ and (bme-dach) $\text{Fe}(\text{NO})$ readily react with excess NO gas in MeOH to form red-brown derivatives with $\nu(\text{NO})$ absorptions of 1780, 1755 cm^{-1} . With typical

(22) (a) Enemark, J. H.; Feltham, R. D. *Coord. Chem. Rev.* **1974**, 340–404. (b) Enemark, J. H.; Feltham, R. D. *J. Chem. Soc., Dalton Trans.* **1972**, 718–722.

(23) Noguchi, T.; Hoshino, M.; Tsujimura, M.; Odaka, M.; Inoue, Y.; Endo, I. *Biochemistry* **1996**, 35, 16777–16781.

(24) Chatel, S.; Chauvin, A.-S.; Tuchagues, J.-P.; Leduc, P.; Bill, E.; Chottard, J.-C.; Mansuy, D.; Artaud, I. *Inorg. Chem. Acta* **2002**, 336, 19–28.

(25) Karlin, K. D.; Rabinowitz, H. N.; Lewis, D. L.; Lippard, S. J. *Inorg. Chem.* **1977**, 16, 3262–3267.

(26) Vogel, K. M.; Kozłowski, P. M.; Zgierski, M. Z.; Spiro, T. G. *J. Am. Chem. Soc.* **1999**, 121, 9915–9921.

(27) Scheidt, W. R.; Duval, H. F.; Neal, T. J.; Ellison, M. K. *J. Am. Chem. Soc.* **2000**, 122, 4651–4659.

(28) Kini, A. D.; Washington, J.; Kubiak, C. P.; Morimoto, B. H. *Inorg. Chem.* **1996**, 35, 6904–6906.

(29) Ellison, M. K.; Schedit, W. R. *Inorg. Chem.* **1998**, 37, 382–383.

Table 2. Crystallographic Data for the (N₂S₂)Fe(NO) Complexes

	(bme*-daco)Fe(NO) ^a	(bme-dach)Fe(NO) ^a	(bme-daco)Co(NO) ^a	(bme-pda)Co(NO) ^a
formula	C ₁₄ H ₂₈ FeN ₃ OS ₂	C ₉ H ₁₈ FeN ₃ OS ₂	C ₁₀ H ₂₀ CoN ₃ OS ₂	C ₉ H ₂₀ CoN ₃ OS ₂
fw (g/mol)	374.36	304.23	321.34	309.23
cryst syst	monoclinic	triclinic	monoclinic	monoclinic
space group	C2/c	P1	P2(1)/n	P2(1)/c
unit cell				
a (Å)	21.211(4)	7.3544(9)	7.697(4)	8.2608(13)
b (Å)	7.4354(14)	8.0686(10)	23.622(12)	12.7516(19)
c (Å)	24.245(5)	11.6108(14)	7.705(4)	12.5833(19)
α (deg)	90	95.523(2)	90	90
β (deg)	113.095(3)	97.570(2)	112.703(8)	98.676(2)
γ (deg)	90	114.273(2)	90	90
V (Å ³)	3517.3(12)	613.92(13)	1292.2(11)	1310.3(3)
Z	8	2	4	4
R1 ^b , wR2 ^c (%) [I > 2σ(I)]	3.85, 9.85	3.42, 8.69	5.93, 10.44	2.20, 5.28
R1 ^b , wR2 ^c (%) all data	4.05, 10.09	3.53, 8.82	7.44, 10.98	2.31, 5.35

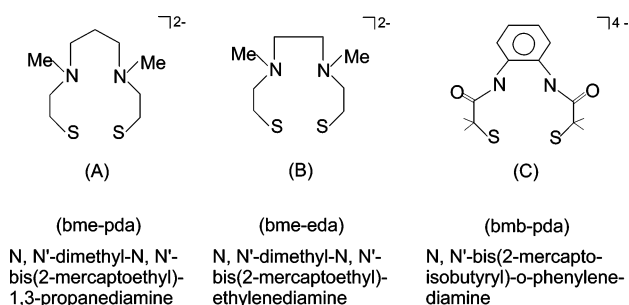
^a Obtained using graphite-monochromatized Mo Kα radiation (λ = 0.71073 Å) at 110 K. ^b R1 = Σ||F_o| - |F_c||/ΣF_o. ^c wR2 = [Σ[w(F_o² - F_c²)²]/Σw(F_o²)^{1/2}].

RS⁻ ligands, such ν(NO) bands in the 1750–1780 cm⁻¹ region are characteristic of Roussin's red "ester", (μ-SR)₂[Fe(NO)₂]₂, a ubiquitous side product of all thiolate-iron nitrosyls in excess NO.^{33,34} These products have not been isolated, and their exact nuclearity is as of now unknown. Earlier studies of iron nitrosyls and a bidentate dithiolate found a tetranuclear structure containing a dimer of Roussin's red, an analogue of which is a possibility with the N₂S₂ dithiolate ligands.⁸

Vis-UV Spectra. As previously reported for the (bme-pda)Fe(NO) and (bme-eda)Fe(NO) complexes, **1**, **2**, and **3** have charge-transfer bands in the ~220–350 nm range and a d-d transition band at ~630 nm in the vis-UV spectra.²⁵

Molecular Structures from X-Ray Crystallography. Crystals of complexes **2** and **3** were obtained by vapor diffusion of pentane into CH₂Cl₂ solutions at 5 °C. For complexes **4** and **5**, a solvent-layering technique was used. Crystallographic data for the structures are given in Table 2. The molecular structures of complexes **2**, **3**, **4**, and **5** are shown in Figures 2 and 3 as 50% thermal ellipsoid plots. Selected bond distances, angles, and atom displacements from planes are given in Table 3; full listings are given in Supporting Information. For comparison, data for complex **1** and the (bme-pda)Fe(NO) complex of Lippard et al.⁷ are also listed in Table 3.

The structures of all the N₂S₂M(NO) (M = Fe, Co) complexes are approximately square pyramids with the M residing above an N₂S₂ plane and capped by an apical NO


Figure 2.

group. The displacement of iron from the best N₂S₂ plane is ca. 0.48 Å in the diazacycle derivatives and slightly less in the open-chain bme-pda derivative (0.41 Å). The cobalt displacement is even less, 0.31–0.37 Å. The molecular structures of complexes **3**, **4**, and **5** show disorder in the NO group; for the latter two, that disorder is torsional in character; for complex **3**, the disorder is also in the ∠Fe–N–O angles, refined to be 152.4(6)^o and 144(3)^o. The ∠Fe–N–O = 148.7(2)^o in complex **2** is similar to that of complex **1**, 151.7(5)^o.⁸ A feature apparently common to all structures of this type is the orientation of the NO bond-vector toward the thiolate region of the N₂S₂ donor set. In fact, the dihedral angles defined by the intersection of N–M–S and O–N–M planes are typically less than 20^o, Figure 5. For complex **2**, which shows no M–NO torsional disorder, the NO bond vector largely eclipses the Fe–S bond vector!

All structural features of the mesocyclic ligand derivatives are typical of this class of N₂S₂ ligands, and metric (distance) data are unremarkable. The iron-to-nitrogen distance of Fe–NO averages to 1.71 Å in (N₂S₂)Fe(NO) (N₂S₂ = bme-daco, bme*-daco, and bme-dach) and is 1.70 Å in the open-chain analogue, (bme-pda)Fe(NO). An interesting difference between the diazacycle complexes vs the open chain derivatives is the reversal in ∠N–Fe–N and ∠S–Fe–S angles. For complexes **1**, **2**, and **3**, the former is smaller than the latter with a major difference arising in the dach derivative. That is, the 2-carbon N-to-N link pinches the ∠N–Fe–N angle to 79^o and opens the ∠S–Fe–S angle to 95^o, see Supporting Information, Figure S1. In contrast, the open-chain derivatives for both Fe and Co find the N–M–N

(30) Schedit, W. R.; Frisse, M. E. *J. Am. Chem. Soc.* **1975**, *97*, 17–21.

(31) Schedit, W. R.; Duval, F. Neal, T. J.; Ellison, M. K. *J. Am. Chem. Soc.* **2000**, *122*, 4651–4659.

(32) Schedit, W. R.; Hoard, J. L. *J. Am. Chem. Soc.* **1973**, *95*, 8281–8288.

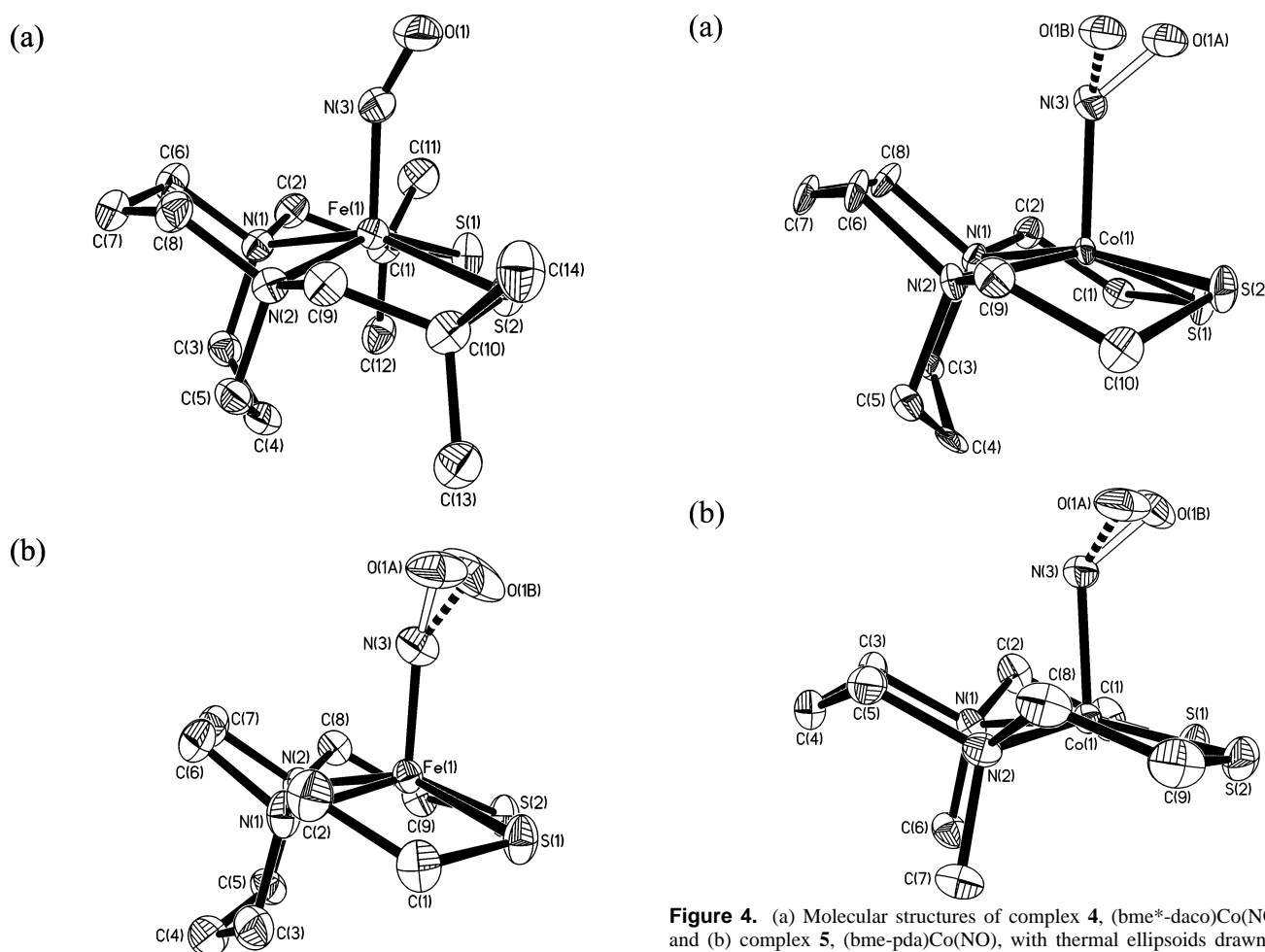
(33) (a) Butler, A. R.; Glidewell, C.; Johnson, I. L.; Walton, J. C. *Polyhedron* **1987**, *6*, 2085–2090. (b) McDonald, C. C.; Phillips, W. D.; Mower, H. F. *J. Am. Chem. Soc.* **1965**, *87*, 3319–3326. (c) Basosi, R.; Gaggelli, E.; Tiezzi, E.; Valensin, G. *J. Chem. Soc., Perkin Trans. 2* **1975**, 423–428. (d) Jezowska-Trzebiatowska, B.; Jezierski, A. *J. Mol. Struct.* **1973**, *19*, 635–640. (e) Bryar, T. R. Eaton, D. R. *Can. J. Chem.* **1992**, *70*, 1917–1926.

(34) (a) Thomas, J. T.; Robertson, J. H.; Cox, E. G. *Acta Crystallogr.* **1958**, *11*, 599–604. (b) Glidewell, C.; Lambert, R. J. *J. Chem. Soc., Dalton Trans.* **1989**, 2061–2064. (c) Glidewell, C.; Harman, M. E.; Bursthouse, M. B.; Johnson, I. L.; Motevalli, M. *J. Chem. Res. (S)* **1988**, 212–213(M), 1676–1690. (d) Cai, J.; Mao, S. *Jiegou Huaxue* **1983**, *2*, 263–267.

Table 3. Selected Distances and Angles of Complexes **1**, (bme-daco)Fe(NO); **2**, (bme*-daco)Fe(NO); **3**, (bme-dach)Fe(NO); **4**, (bme-daco)Co(NO); **5**, (bme-pda)Co(NO); and L'Fe(NO)^a

compound	1	2	3	L'Fe(NO) ^a	4	5
M–S (Å)	2.239(2)	2.2105(7)	2.2172(7)	2.240(3)	2.2152(17)	2.2115(5)
	2.253(2)	2.2408(7)	2.2456(7)	2.209(3)	2.2339(16)	2.2180(5)
M–N(N ₂ S ₂)	2.069(5)	2.0599(18)	2.0001(2)	2.082(7)	2.036(4)	2.2094(14)
	2.072(5)	2.0816(18)	2.025(2)	2.093(8)	2.041(4)	2.20598(13)
M–NO (Å)	1.707(6)	1.714(2)	1.705(2)	1.697(9)	1.765(4)	1.7818(14)
N–O (Å)	1.094(4)	1.174(3)	1.167(18)	1.146(9)	1.173(7)	1.164(10)
			1.23(3)		1.160(16)	1.148(5)
M(N ₂ S ₂) disp ^b	0.4839	0.4792	0.4896	0.414	0.3717	0.3078
N(1) _(N₂S₂) disp ^c	−0.0765	−0.0174	−0.0601	0.0145	−0.0448	−0.1310
N(2) _(N₂S₂) disp ^c	0.0762	0.0175	0.0600	−0.0146	0.0447	0.1298
S(1) _(N₂S₂) disp ^c	−0.0700	0.0164	0.0468	−0.0146	0.0451	0.1192
S(2) _(N₂S₂) disp ^c	0.0697	−0.0164	−0.0467	0.0147	−0.0450	−0.1180
∠N–M–N(N ₂ S ₂)	86.99(19)°	87.65(8)°	79.03(9)°	94.1(3)°	87.91(17)°	95.80(5)°
∠N–M–N(NO)	101.76°	101.75°	101.97°	98.5°	97.5°	94.20°
∠M–N–O	151.7(5)°	148.74(17)°	152.4(6)°	155.2°	129.6(8)°	130.1(3)°
			144(3)°		128.7(4)°	126.7(10)°
∠S–M–S	88.11(8)°	86.32(3)°	94.91(3)°	86.4(1)°	88.63(7)°	85.75(2)°

^a See Figures 3 and 4 for molecular structures. L' = bme-pda, see ref 7. ^b disp is defined as the displacement of Fe from the best N₂S₂ plane. ^c N and S atoms displacements from the best N₂S₂ planes.

**Figure 3.** (a) Molecular structures of complex **2**, (bme*-daco)Fe(NO), and (b) complex **3**, (bme-dach)Fe(NO), with thermal ellipsoids drawn at 50% probability level.

angles at 99° and 94°, respectively, while the S–M–S angle is contracted to 86° in both.

The packing diagrams of complexes **1–3** show obvious alignments of hydrophobic and hydrophilic regions. Thus, the NO ligands lie between two adjacent Fe(NO) complexes

Figure 4. (a) Molecular structures of complex **4**, (bme*-daco)Co(NO), and (b) complex **5**, (bme-pda)Co(NO), with thermal ellipsoids drawn at 50% probability level.

with O···O separations of 3.4 and 5.2 Å for complex **1**; 5.1 and 6.2 Å for complex **2**; and 3.6 and 4.5 Å for complex **3**. These may be seen by viewing down the *b* axis and with the *a* axis horizontal to the plane of paper (see Supporting Information, Figure S2). There are no obvious close intermolecular interactions that might suggest a packing force influence on the distinctive NO orientation over the M–S bond vector.

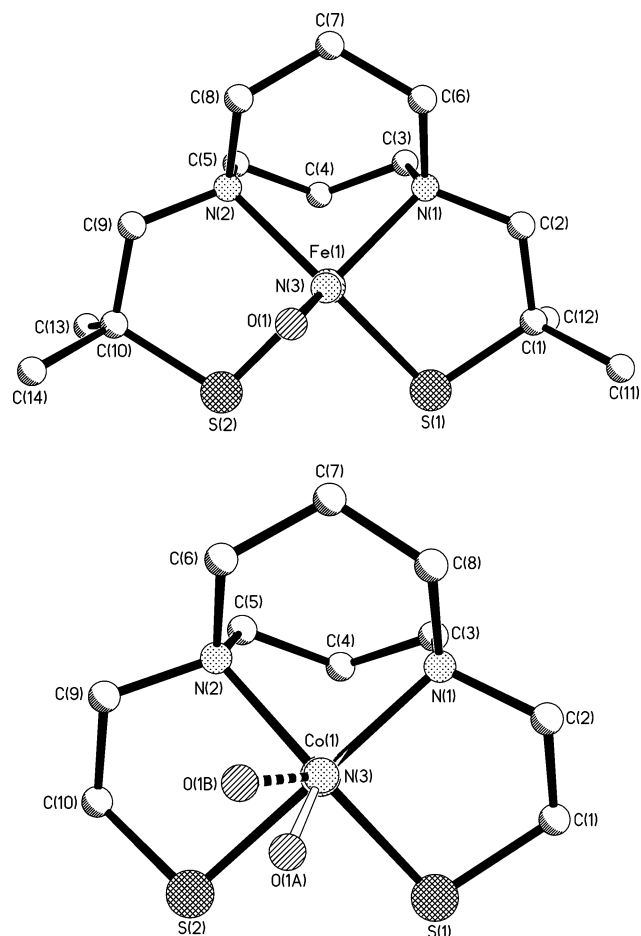


Figure 5. Vertical view (eclipsing N and M of M–NO unit) of ball-and-stick structures of (bme*-daco)Fe(NO) and (bme-daco)Co(NO).

Magnetism and EPR Data. Complexes **1**, **2**, and **3** are paramagnetic and show a single isotropic signal in their EPR spectra with g values of 2.05, 2.04, and 2.05, respectively. Figure 6 displays the room-temperature spectra of (bme*-daco)Fe(NO), complex **2**, and (bme-dach)Fe(NO), complex **3**. The former shows ^{14}N hyperfine coupling resulting in a triplet with hyperfine coupling 12.2 G, which is evidence for the residence of the odd electron in a molecular orbital with substantial NO character and delocalization within the {Fe(NO)}⁷ moiety. These EPR g values and hyperfine couplings have also been observed for the (bme-pda)Fe(NO) and (bme-eda)Fe(NO) complexes.^{7,25} Interestingly, the Fe–porphyrin nitrosyl complex, (TPP)Fe(NO), in toluene has an almost identical signal, a triplet with g values around 2.05 and hyperfine coupling from ^{14}N of 17.4 G.³⁵ While the spectrum of **3** does not show distinct hyperfine coupling, the irregular shape of the resonance is possibly due to a mixture of isomeric forms derived from NO binding on either side of the N_2S_2 plane (the 2-carbon or 3-carbon atom N-to-N linked side). The cobalt complexes, **4** and **5** of E–F notation {Co(NO)}⁸, as well as the analogous cobalt porphyrin nitrosyl complexes, are diamagnetic and EPR silent.^{36,37}

(35) Wayland, B. B.; Olson, L. W. *J. Am. Chem. Soc.* **1974**, *96*, 6037–6041.

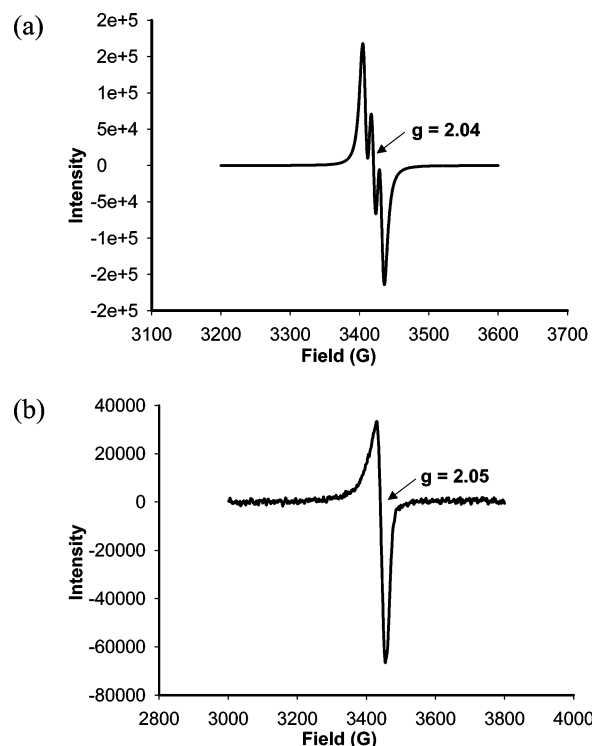


Figure 6. EPR spectra of (a) complex **2** and (b) complex **3** at 298 K in CH_2Cl_2 solution.

Electrochemical Studies. The cyclic voltammograms (CVs) of the (N_2S_2) $M(NO)$ compounds ($M = \text{Fe}, \text{Co}$; $N_2S_2 = \text{bme-dach}, \text{bme-daco}, \text{bme-pda}, \text{bme}^*\text{-daco}$) were examined at room temperature in CH_2Cl_2 containing 0.1 M $n\text{-Bu}_4\text{-NPF}_6$ with a glassy carbon working electrode. The complete CVs at 200 mV/s scan rate are presented in Figures 7 and 8, and potential and reversibility data from CVs are given in Table 4.

As seen in Figure 7a, the (bme-dach)Fe(NO) complex undergoes one reversible reduction at $E_{1/2} = -1.13$ V and one irreversible oxidation at $E_{\text{pa}} = 0.52$ V within the solvent window. The separation in peak potentials, $\Delta E_{\text{p}} = |E_{\text{pa}} - E_{\text{pc}}|$ for the reduction at $E_{1/2} = -1.13$ V is 182 mV, and this value is comparable to that determined for the $\text{Cp}^*\text{Fe}/\text{Cp}^*\text{Fe}^+$ couple used as an internal reference. In addition, the anodic-to-cathodic peak current ratio ($i_{\text{pa}}/i_{\text{pc}}$) for this reduction is 0.87, indicative of the chemically reversible reduction. Furthermore, as indicated by linearity in the plot of i_{pc} vs $\nu^{1/2}$, this reduction process is diffusion-controlled. Hence, the overall electrochemical data suggest that the reduction at $E_{1/2} = -1.13$ V is a diffusion-controlled, chemically reversible, one-electron-transfer process.

Similar redox behaviors have been observed for the previously reported neutral four-coordinate (N_2S_2)Ni complexes. For example, (bme-dach)Ni undergoes one reversible reduction at ca. -1.9 V and one irreversible oxidation at ca. 0.36 V (referenced to $E_{1/2}$ of $\text{Cp}_2\text{Fe}/\text{Cp}_2\text{Fe}^+ = 400$ mV) in CH_3CN solution. These processes have been assigned to the one-electron $\text{Ni}^{\text{II}}/\text{Ni}^{\text{I}}$ couple (eq 1), and the oxidation of thiolate to the thiyl radical, respectively.³⁸ As the N_2S_2 ligands are not expected to be easily reduced, the reduction activity for the (N_2S_2) $M(NO)$ complexes are presumed to occur at

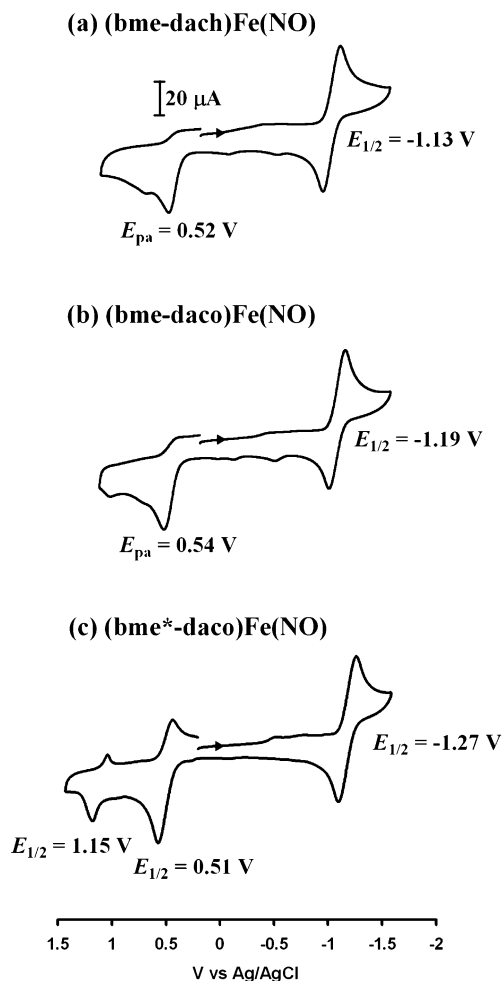
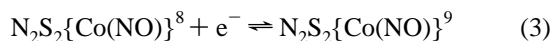
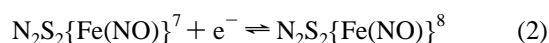
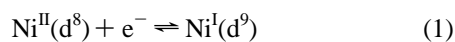


Figure 7. CVs of 2.0 mM CH_2Cl_2 solution of (a) (bme-dach)Fe(NO), (b) (bme-daco)Fe(NO), and (c) (bme*-daco)Fe(NO) in 0.1 M $n\text{-Bu}_4\text{NPF}_6$ with a glassy carbon electrode at scan rate of 200 mV/s. All potentials are reported relative to Ag/AgCl electrode using $\text{Cp}^*_2\text{Fe}/\text{Cp}^*_2\text{Fe}^+$ as reference ($E_{1/2} = 0.00$ V vs Ag/AgCl in CH_2Cl_2).

the M(NO) moiety. Thus, for the (bme-dach)Fe(NO) complex, the reduction at $E_{1/2} = -1.13$ V is reasonably assigned to metal-nitrosyl-centered reduction (eq 2), whereas the process at $E_{\text{pa}} = 0.52$ V is assigned to sulfur-based oxidation.



Shown in Figure 7, the CV of (bme-daco)Fe(NO) also reveals redox processes similar to those of the (bme-dach)-Fe(NO) complex, whereas the (bme*-daco)Fe(NO) complex undergoes one reversible reduction and two partially reversible oxidations. The cathodic $E_{1/2}$ value observed for (bme-daco)Fe(NO) differs little from the (bme-dach)Fe(NO);

(36) Scheidt, W. R.; Hoard, J. L. *J. Am. Chem. Soc.* **1973**, *95*, 8281–8288.

(37) Richter-Addo, B. B.; Hodge, S. J.; Yi, G.-B.; Khan, M. A.; Ma, T.; Caemelbecke, E. V.; Guo, N.; Kadish, K. M. *Inorg. Chem.* **1996**, *35*, 6530–6538.

(38) Farmer, P. J.; Reibenspies, J. H.; Lindahl, P. A.; Darensbourg, M. Y. *J. Am. Chem. Soc.* **1993**, *115*, 4665–4674.

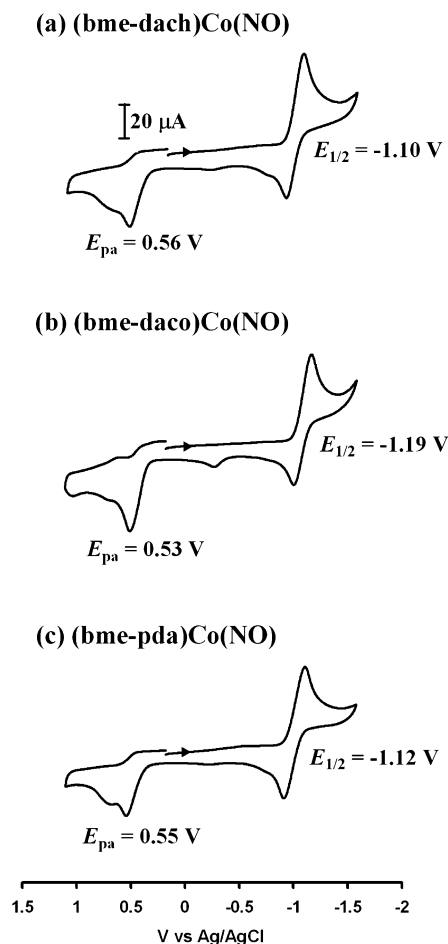


Figure 8. CVs of 2.0 mM CH_2Cl_2 solution of (a) (bme-dach)Co(NO), (b) (bme-daco)Co(NO), and (c) (bme*-pda)Co(NO) in 0.1 M $n\text{-Bu}_4\text{NPF}_6$ with a glassy carbon electrode at scan rate of 200 mV/s. All potentials are reported relative to Ag/AgCl electrode using $\text{Cp}^*_2\text{Fe}/\text{Cp}^*_2\text{Fe}^+$ as reference ($E_{1/2} = 0.00$ V vs Ag/AgCl in CH_2Cl_2).

Table 4. Potential and Reversibility Data from Cyclic Voltammetry for $(\text{N}_2\text{S}_2)\text{M}(\text{NO})$ (M = Co, Fe) Compounds in CH_2Cl_2 , 0.1 M $n\text{-Bu}_4\text{NPF}_6$ at a 200 mV/s Scan Rate

compound	reduction		oxidation	
	$E_{1/2}$ (V) (ΔE (mV)) ^b	$i_{\text{pa}}/i_{\text{pc}}$	first oxidn	second oxidn
(bme-dach)Fe(NO)	-1.13 (182)	0.87	0.52	
(bme-daco)Fe(NO)	-1.19 (176)	0.84	0.54	
(bme*-daco)Fe(NO)	-1.27 (173)	0.87	0.51 ^c	1.15 ^d
(bme-dach)Co(NO)	-1.10 (160)	0.82	0.56	
(bme-daco)Co(NO)	-1.19 (185)	0.70	0.53	
(bme-pda)Co(NO)	-1.12 (198)	0.82	0.55	
(bme*-daco)Co(NO)	-1.28 (162)	0.74	0.50 ^e	1.25

^a All potentials are reported relative to Ag/AgCl reference electrode using $\text{Cp}^*_2\text{Fe}/\text{Cp}^*_2\text{Fe}^+$ as reference ($E_{1/2} = 0.00$ V vs Ag/AgCl in CH_2Cl_2).

^b Instrumental iR compensation was not used to minimize the uncompensated iR drop in the solution. The separation in peak potentials is comparable to that determined for the $\text{Cp}^*_2\text{Fe}/\text{Cp}^*_2\text{Fe}^+$ couple used as an internal reference.

^c This value is for half-potential ($E_{1/2}$) (ΔE (mV) = 130, $i_{\text{pc}}/i_{\text{pa}} = 0.53$).

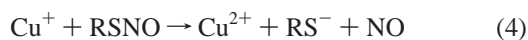
^d This value is for half-potential ($E_{1/2}$) (ΔE (mV) = 140, $i_{\text{pc}}/i_{\text{pa}} = 0.59$).

^e This value is for half-potential ($E_{1/2}$) (ΔE (mV) = 114, $i_{\text{pc}}/i_{\text{pa}} = 0.36$).

however, the $E_{1/2}$ (cathodic) for (bme*-daco)Fe(NO) is significantly more negative. The latter result is consistent with the greater electron-donating ability of the thiolate sulfurs which have gem-dimethyl groups. Such an observation was noted in comparisons of the $\text{Ni}^{\text{II/I}}$ couple in (bme-daco)Ni (ca. -1.9 V) vs (bme*-daco)Ni (ca. -2.1 V) in

CH₃CN solution.³⁸ It is also noteworthy that the first oxidation events for the three (N₂S₂)Fe(NO) compounds show little difference and no recognizable trend. As these oxidations are assumed to be sulfur-based, such a result is not unexpected. The CVs of the analogous (N₂S₂)Co(NO) complexes are shown in Figure 8. In general, all the (N₂S₂)Co(NO) compounds undergo redox processes similar to those of the (N₂S₂)Fe(NO) complexes. For example, the CV of the (bme-dach)Co(NO) complex reveals one reversible reduction at $E_{1/2} = -1.10$ V and one irreversible oxidation at $E_{pa} = 0.56$ V. As in the case of (N₂S₂)Fe(NO), these redox processes are also assigned to metal-nitrosyl-centered reduction (eq 3) and sulfur-based oxidation, respectively. Interestingly, the (bme*-daco)M(NO) complexes display two oxidation events whereas all other complexes show only one. As these have gem-dimethyl groups, the possibility of sequential production of stabilized thiyl radicals should be further explored. Yet another notable feature discovered in the electrochemical studies is the fact that redox potentials observed for (N₂S₂)Co(NO) are almost identical to those of (N₂S₂)Fe(NO) containing the corresponding N₂S₂ ligand. This result is remarkable given the differences in $\nu(\text{NO})$ values and M–N–O angles for Co vs Fe.

Chemical Reactivity. Aspects of the reactivity of the [(N₂S₂)Fe]₂ and (N₂S₂)Fe(NO) complexes were studied as follows. As nitrosothiols (RSNOs) are considered to be NO transfer agents in biological systems, the potential for [(bme*-daco)Fe]₂ to serve as an NO acceptor from the stable nitrosothiol Ph₃CSNO was explored. Thus, 1:1 mixtures in CH₂Cl₂ solutions at room temperature were monitored by IR spectroscopy. Over the course of 4 days in the dark or following exposure to strong sunlight for 5 h, the IR spectra showed no evidence of NO transfer yielding the (N₂S₂)Fe(NO). On addition of [Cu(CH₃CN)₄]BF₄, however, there was an immediate color change from brown-green to dark brown-red. After overnight stirring, the solvent was removed by vacuum and the residue was redissolved in CH₂Cl₂. The solution IR showed a $\nu(\text{NO})$ absorbance at 1648 cm⁻¹, indicating formation of (bme*-daco)Fe(NO). This result is consistent with the known Cu(I)-catalyzed decomposition of nitrosothiols (RSNOs) to release NO and form disulfide compounds in solution (eqs 4–6).³⁹ Thus, the formation of the (bme*-daco)Fe(NO) results from the copper-catalyzed production of free NO in solution. Similar results were obtained for [(bme-daco)Fe]₂.



For comparison to iron porphyrin complexes which are known to react with NO₂⁻ to form porphyrin iron nitrite complexes,⁴⁰ we examined the reaction of [(bme-daco)Fe]₂

and [PPN][NO₂] in MeOH solution. The brown solution darkened, and an $\nu(\text{NO})$ absorption at 1670 cm⁻¹, assigned to (bme-daco)Fe(NO), developed in the IR spectra over the course of 4.5 h. No further IR changes occurred after 16 h of stirring. The product was isolated in low yield (<10%), and no optimization was attempted.

As the photolability of NO-deactivated NHase is an important characteristic of the natural N₂S₂Fe(NO) complex in the nitrile hydratase active site, we attempted photolysis of the (N₂S₂)Fe(NO) complexes in MeOH solutions in Pyrex glass using a Hg-vapor lamp. The vis–UV spectral monitor of this mixture found the same position and intensity of bands after a 4 h photolysis reaction (see Supporting Information, Figure S3). The stability of the (N₂S₂)Fe(NO) complex under stringent photolysis conditions is consistent with properties of iron mononitrosyl complexes synthesized by Mascharak, Kovacs, Artaud, and Grapperhaus et al.^{1a,1b,41} From their studies, it has been proposed that a thiolate ligand trans to NO is a requirement for the observed photolability of Fe–NHase.^{1a,1b,41}

The NO-inactivated Fe–NHase active site structure shows two cysteine sulfurs are post-translationally modified to sulfinate (RSO₂⁻) and sulfenate (RSO⁻).^{1,10a} As the sulfinate and sulfenate may play a key role in hydration of nitrile in NHase¹ and as the nickel-bound N₂S₂ ligands based on diazacycles bme-daco and bme-dach readily form S-oxygenates,^{3d,3f} the potential for oxygen uptake by sulfur in the (N₂S₂)Fe(NO) complexes was explored. In fact, there was observed no color or IR spectral changes following an overnight O₂ gas purge of a CH₂Cl₂ solution of (bme-daco)Fe(NO). Further attempts to produce sulf-oxygenated products with pressures of O₂, or O-atom sources such as 4-chloropyridine oxide, or H₂O₂ in CH₂Cl₂ or MeOH gave either negative results or decomposition to insoluble compounds. Studies by Mascharak et al.^{1b} provide evidence that carboxamido nitrogens as in the natural Cys–Ser–Cys, tetraanionic N₂S₂ ligand of NHase are required to stabilize Fe³⁺ sulfinate and sulfenate.^{1b} It should be mentioned that direct reaction of [(N₂S₂)Fe^{II}]₂ dimers with molecular O₂ or pyridine oxide results in formation of (μ -oxo)[(N₂S₂)Fe^{III}]₂ complexes.^{3e} That is, Fe-based oxygenation is preferred over S-oxygenation, and in the NO-bound form, the (N₂S₂)Fe is protected from O₂ sensitivity.

Conclusions and Comments

The (N₂S₂)M(NO) complexes (N₂S₂ = bme-daco, bme*-daco, bme-dach; M = Fe, Co) can be directly synthesized by reaction of [(N₂S₂)M]₂ with NO gas, producing thermally stable, non-photolabile complexes indicating the predilection of the N₂S₂ donor set for such MNO moieties. Solid-state structures have shown that all (N₂S₂)M(NO) complexes are in square pyramidal geometry, with the M displaced out of the N₂S₂ planes by 0.3 (Co) to 0.5 (Fe) Å. The bent M–N–O

(39) (a) Williams D. L. H. *Chem. Commun.* **1996**, 32, 1085–1091. (b) Al-Sa'doni, H.; Ferro, A. *Clin. Sci.* **2000**, 98, 507–520. (c) Lee, J.; Chen, L.; West, A. H.; Richter-Addo, G. B. *Chem. Rev.* **2002**, 102, 1019–1066.

(40) (a) Nasri, H.; Wang, Y.; Huynh, B. H.; Schedit, W. R. *J. Am. Chem. Soc.* **1991**, 113, 717–719. (b) Finnegan, M. G.; Lappin, A. G.; Schedit, W. R. *Inorg. Chem.* **1990**, 29, 181–185. (c) Wei, Z.; Ryan, M. D. *Inorg. Chim. Acta* **2001**, 314, 49–57. (d) Wolak, M.; Eldik, R. V. *Coord. Chem. Rev.* **2002**, 230, 262–282 and references therein.

apexes are oriented toward the sulfur atoms with a distinctive and, as of now, unexplained alignment of the NO bond vector over one M–S bond. To our knowledge, the X-ray diffraction studies of the (N₂S₂)Co(NO) complexes reported here are only the second and third for such neutral compounds while several are known for the N₂S₂–iron mononitrosyl complexes.⁴³ The ∠Fe–N–O bond angles are in the range of 144–152°. In contrast, the cobalt nitrosyl analogues show a greater bend, with a ∠Co–N–O angle of 127–130° consistent with a more-electron-rich configuration, {Co(NO)}⁸ as compared to {Fe(NO)}⁷. A reasonable expectation is that the diamagnetic cobalt complex expresses a major contribution from a Co^{III}–(NO[−]) configuration, and the paramagnetic iron complex is represented by Fe^{II}–(NO•). While the infrared spectra are in agreement with this assignment, with ν(NO) values of the (N₂S₂)Co(NO) compounds some 50 cm^{−1} lower than the analogous (N₂S₂)Fe(NO) derivatives, the electrochemical data present a conundrum. The reduction potentials, assigned to {Co(NO)}⁸ + e[−] ⇌ {Co(NO)}⁹ or {Fe(NO)}⁷ + e[−] ⇌ {Fe(NO)}⁸ are very similar, and in cases identical, for most members of the series. Furthermore, at −1.10 to −1.20 V, the reduction events are ca. 1 V more positive than that of analogous neutral N₂S₂Ni complexes which show the Ni^{II}(d⁸) + e[−] ⇌ Ni^I(d⁹) couple at −1.9 to −2.1 V. The latter can be explained by the poor electron affinity of the single metal-based reduction as contrasted to the electron-delocalization possible in the M–NO moieties. That the reduction potentials of the {Co(NO)}⁸ and {Fe(NO)}⁷ species should be so close was not, a priori, predictable.

All aspects of the structures and physical properties of the (N₂S₂)M(NO) compounds indicate the great similarities of Co and Fe within this coordination environment, consistent with the presence in nature of two metallic forms of nitrile

- (41) Grapperhaus, C. A.; Li, M.; Patra, A. K.; Poturovic, S.; Kozlowski, P. M.; Zgierski, M. Z.; Mashuta, M. S. *Inorg. Chem.* **2003**, *42*, 4382–4388.
- (42) Chatel, S.; Rat, M.; Dijols, S.; Leduc, P.; Tuchagues, J. P.; Mansuy, D.; Artaud, I. *J. Inorg. Biochem.* **2000**, *80*, 239–246.
- (43) McCleverty, J. A. *Chem. Rev.* **2004**, *104*, 403–418.

hydratase. In agreement with the conclusion of Artaud et al.,⁴² there is no obvious barrier to the binding of NO in cobalt–NHase as is found in the deactivated form of iron–NHase. An argument to the contrary can, of course, be based on the fact that the dianionic N₂S₂ analogues in this study result in neutral complexes in which the metals are in a more reduced state than in the NHase which derive from tetraanionic ligands, containing carboxamido nitrogens, stabilizing oxidized Fe(NO) states, and apparently promoting the sulfoxidation that was not observed here.

Finally, the similarity between the (porphyrin)M(NO) derivatives and the (N₂S₂)M(NO) complexes herein, established through comparisons of EPR spectral properties, magnetism, and ν(NO) IR data, is of note.⁴³ In view of the enormous influence of porphyrins as a class of ligands in coordination and bioinorganic chemistry, further studies of the scope of the N₂S₂ ligands and their potential for various applications as have been appropriate for N₄ porphyrins is warranted.

Acknowledgment. The authors acknowledge the financial support of the National Science Foundation (Grant No. CHE 01-11629 to M.Y.D. for this work, Grant No. CHE 00-92010 for the EPR instrument, and Grant No. CHE 98-07975 for the purchase of X-ray equipment) and contributions from the Robert A. Welch Foundation. Texas A&M University Chemistry Laboratory, CHEM 433, supported the contributions of C. Dalrymple and M. C. Sarahan in an extended laboratory project.

Supporting Information Available: Tables of crystal data and experimental conditions for the X-ray studies, atomic coordinates, and *B*_{eq} values, complete listings of bond lengths and bond angles, and anisotropic temperature factors for complexes **2**, **3**, **4**, and **5**. This material is available free of charge via the Internet at <http://pubs.acs.org>.

Note Added after ASAP Publication. This article was released ASAP on October 18, 2005, with errors in Figure 1. The correct version was posted October 31, 2005.

IC051027S